doi:10.1016/j.jmb.2010.06.037 J. Mol. Biol. (2010) 401, 532–543

JMB

Available online at www.sciencedirect.com

ScienceDirect

ELSEVIER

Equivalent Mutations in the Eight Subunits of the Chaperonin CCT Produce Dramatically Different Cellular and Gene Expression Phenotypes

Maya Amit[1], Sarah J. Weisberg[1], Michal Nadler-Holly[1], Elizabeth A. McCormack[2], Ester Feldmesser[3], Daniel Kaganovich[4], Keith R. Willison[2] and Amnon Horovitz[1]*

[1]*Department of Structural Biology, Weizmann Institute of Science, Rehovot 76100, Israel*

[2]*Section of Cell and Molecular Biology, Institute of Cancer Research, Chester Beatty Laboratories, London SW3 6JB, UK*

[3]*Department of Biological Services, Weizmann Institute of Science, Rehovot 76100, Israel*

[4]*Department of Biological Chemistry, Weizmann Institute of Science, Rehovot 76100, Israel*

Received 18 March 2010; received in revised form 15 June 2010; accepted 18 June 2010
Available online 25 June 2010

Edited by F. Schmid

The eukaryotic cytoplasmic chaperonin-containing TCP-1 (CCT) is a complex formed by two back-to-back stacked hetero-octameric rings that assists the folding of actins, tubulins, and other proteins in an ATP-dependent manner. Here, we tested the significance of the hetero-oligomeric nature of CCT in its function by introducing, in each of the eight subunits in turn, an identical mutation at a position that is conserved in all the subunits and is involved in ATP hydrolysis, in order to establish the extent of 'individuality' of the various subunits. Our results show that these identical mutations lead to dramatically different phenotypes. For example, *Saccharomyces cerevisiae* yeast cells with the mutation in subunit CCT2 display heat sensitivity and cold sensitivity for growth, have an excess of actin patches, and are the only strain here generated that is pseudo-diploid. By contrast, cells with the mutation in subunit CCT7 are the only ones to accumulate juxtanuclear protein aggregates that may reflect an impaired stress response in this strain. System-level analysis of the strains using RNA microarrays reveals connections between CCT and several cellular networks, including ribosome biogenesis and TOR2, that help to explain the phenotypic variability observed.

Keywords: molecular chaperones; chaperonins; RNA microarrays; structure–function analysis; aggregation

Introduction

Biochemical reactions that take place in eukaryotic cells are often regulated in a more complex fashion than those in prokaryotic cells. The more intricate nature of biochemical regulation in eukaryotes is sometimes manifested in the involvement of hetero-oligomeric protein assemblies in various processes that, in cases of prokaryotes, are mediated by their homo-oligomeric counterparts. For example, the eukaryotic 20S proteosome core particle is made up of seven distinct α subunits and seven distinct β subunits, whereas its prokaryotic functional homologue, the ClpAP protease chaperone machine, consists only of homo-oligomeric rings.[1] Likewise, prokaryotic chaperonins are made up of homo-oligomeric rings, whereas many archaeal chaperonin rings consist of two or three different subunits, and eukaryotic chaperonin rings contain eight distinct subunits.[2] It can be argued that the evolution of hetero-oligomerism is a neutral molecular ratchet effect without functional consequences or, alternatively, that this process does indeed reflect selection for a more complex biochemical behavior. The importance of the hetero-oligomeric nature of

*Corresponding author. E-mail address: Amnon.Horovitz@weizmann.ac.il.

Abbreviations used: CCT, chaperonin-containing TCP-1; FACS, fluorescence-activated cell sorting; GFP, green fluorescent protein; Ubc, ubiquitin conjugating; VHL, von Hippel–Lindau; FDR, false discovery rate; CBP, calmodulin-binding peptide; UTR, untranslated region; PBS, phosphate-buffered saline.

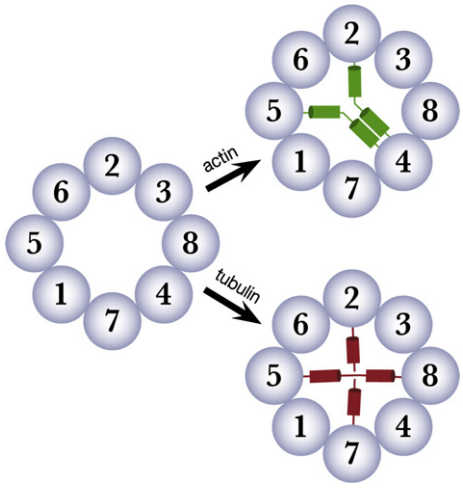

Fig. 1. Modes of binding of actin and tubulin to CCT. Top views showing the order of subunits in CCT[5] and the modes of binding of actin (green) and tubulin (red) to CCT, as determined before.[6,7]

eukaryotic protein complexes for their function under normal and stress conditions has not, however, been rigorously tested. Hence, it is not clear, for example, what the levels of redundancy or moonlighting (i.e., other functions of individual subunits that are carried out not as part of the full complex) are in such assemblies. We explored this issue, in the case of the eukaryotic chaperonin-containing TCP-1 (CCT) described here, by introducing in each subunit in turn an identical mutation at a position that is conserved in all eight subunits in order to establish experimentally the extent of the 'individuality' of function of the various subunits.

CCT is a member of group II chaperonins, found in archaea and in the eukaryotic cytosol, that assists protein folding in an ATP-dependent manner.[3,4] It consists of two back-to-back stacked hetero-octameric rings with a cavity at each end, where protein substrate binding and folding take place. The eight different subunits in each ring are arranged in a defined order around the ring[5] (Fig. 1), which has recently been challenged,[8] and the orientation of the two rings with respect to each other is also fixed.[9] The unique arrangement of subunits in CCT is thought to be essential for proper sequential intra-ring and inter-ring ATP-dependent allosteric communication[10] and for selecting productive substrate-binding modes. For example, only certain modes of interaction (e.g., binding to subunits that are opposite to each other in the ring) may be possible for multidomain substrates, such as actin, that bind simultaneously to more than one subunit, given that the different subunits have distinct substrate specificities.[6,11] Despite their likely functional specializations, the different subunits of CCT have similar amino acid sequences (with a pairwise similarity that ranges from 25% to 35%) and domain architectures.[12] Each subunit consists of three domains: (i) an equatorial domain that contains an ATP binding site; (ii) an apical domain that forms the opening of the central cavity and binds nonfolded polypeptide substrates; and (iii) an intermediate domain that connects the apical and equatorial domains. In this study, we targeted an aspartic acid residue that corresponds to Asp94 in the GDGTTT ATP binding motif in the archaeal chaperonin (the thermosome) from *Thermoplasma acidophilum* and is conserved across species in all eight subunits of CCT and also in GroEL. Asp94 in the thermosome occupies the triphosphate binding site in the absence of nucleotide and is displaced by phosphates upon nucleotide binding.[12] We chose to replace this aspartic acid residue in the different CCT subunits with a glutamic acid in the expectation that these mutations would lead to altered phenotypes but would not be lethal given that the corresponding mutation D87E in GroEL reduces but does not abolish GroEL's ATPase activity.[13] Our results show that these identical mutations in the different CCT subunits lead to dramatically different phenotypes.

Results

Haploid strains of *Saccharomyces cerevisiae* yeast (strain BJ2168), in which the mutation D→E in the

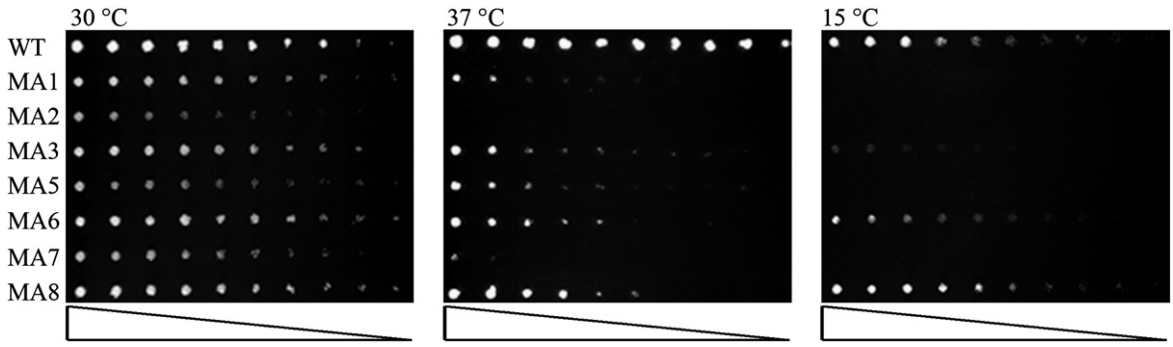

Fig. 2. Effects of the mutations in CCT on cell growth at different temperatures. Nine serial 2-fold dilutions of logarithmic-phase cultures of the different MA cell strains at an OD of 0.5 were carried out (triangles), and 2 μl from each dilution was then transferred to plates containing 300 μg/ml geneticin. The plates were incubated at 15, 30, or 37 °C. See Materials and Methods for more details.

conserved GDGTTT ATP binding motif was introduced into each of the subunits of CCT in turn, were generated by homologous recombination. Throughout the study, strains with these mutations in the chromosomal genes coding for subunits CCT1–CCT8 are designated by MA1–MA8, respectively. Given that an essential function of CCT is to assist the folding of actin and tubulin[3,4,14] and that actin fibers and microtubules have key roles in controlling cell shape and division, we first examined whether the mutations in CCT affect cell growth and morphology and DNA content.

Effects of D→E mutations in CCT on cell growth at different temperatures

The mutations in the different CCT subunits are found to have varying effects on cell growth. The MA4 strain is found to be not viable. The MA2 and MA5 strains are the slowest growers at 30 °C (Fig. 2) with doubling times of 4.5±0.6 and 4.2±0.6 h, respectively, as compared with a doubling time of 2.2±0.8 h in the case of the wild-type strain. The MA1, MA3, MA6, MA7, and MA8 strains grow at 30 °C more slowly than the wild-type strain, but faster than the MA2 and MA5 strains (Fig. 2), with

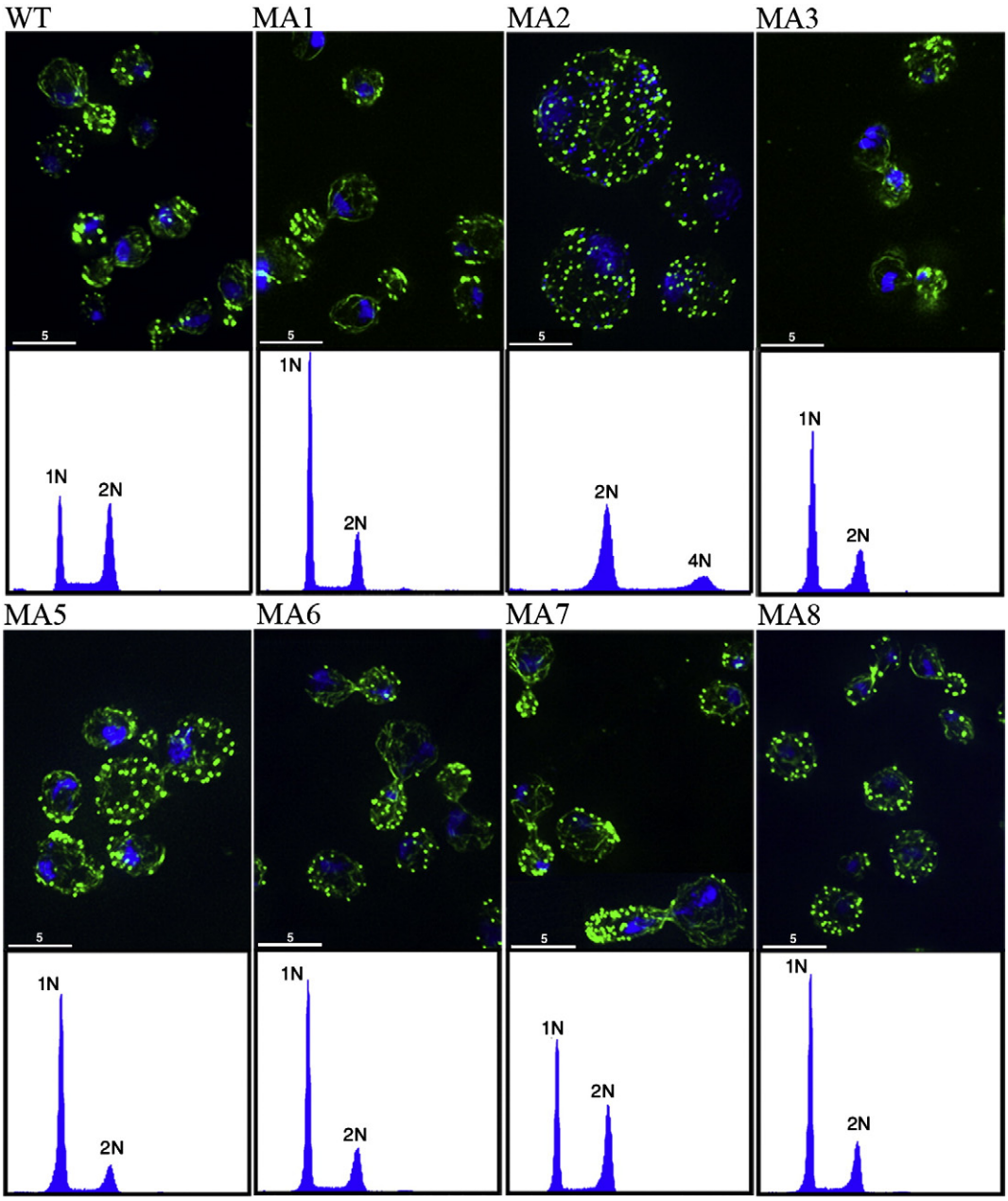

Fig. 3. Effects of the mutations in CCT on cell morphology. Cells from the logarithmic-phase cultures of the different MA strains were subjected to FACS analysis or stained for actin with Alexa Fluor 488 phalloidin (green) and for DNA with 4′,6-diamidino-2-phenylindole (blue) and imaged by fluorescence microscopy. Scale bar represents 5 μm. See Materials and Methods for more details.

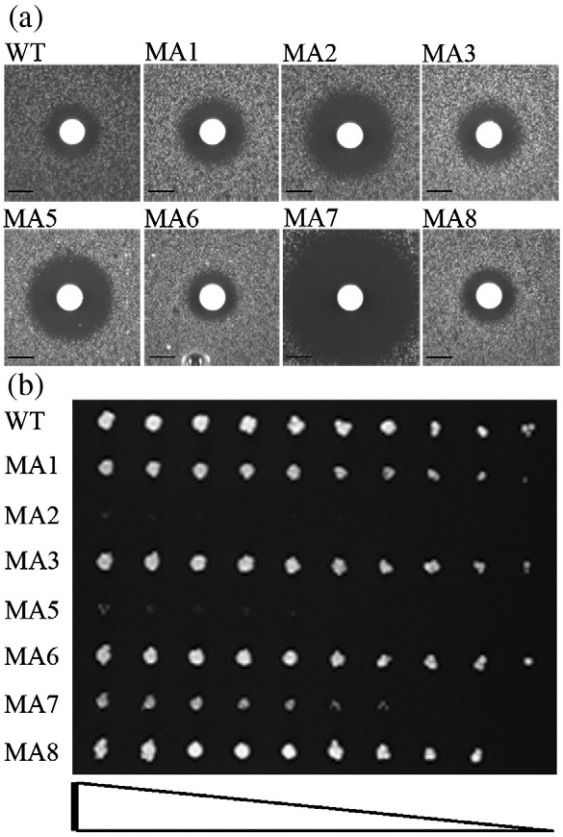

Fig. 4. Sensitivity of the growth of the different MA cell strains to latrunculin-A and benomyl. (a) The effects of latrunculin-A on the growth of the different MA cell strains were monitored using a halo assay. Sterile concentration disks soaked in dimethyl sulfoxide containing 1 mM latrunculin-A were placed on plates previously coated with 4 ml of warm YPD agar media and 10 μl of cultures of the different MA cell strains in logarithmic phase. The plates were incubated at 30 °C for 48 h and then photographed. (b) Nine serial 2-fold dilutions of the logarithmic-phase cultures of the different MA cell strains at an OD of 0.5 were carried out (triangle), and 2 μl from each dilution was then transferred to a plate containing 15 μg/ml benomyl. The plate was incubated at 30 °C for 4 days and then photographed.

respective doubling times of 3.5±0.7, 3.5±0.8, 3.5±0.7, 3.7±0.6, and 3.4±0.6 h, which are quite similar to one another. The temperature sensitivity for growth under heat shock at 37 °C is found to be greatest in the case of the MA2 and MA7 strains, followed by the MA1 strain (Fig. 2). All the other strains also grow less well at 37 °C as compared with the wild-type strain. By contrast, more strains (i.e., MA1, MA2, MA5, and MA7) and, to a somewhat lesser extent, MA3 display similar extreme temperature sensitivities for growth under cold shock at 15 °C. The mutation in MA1 cells (i.e., D96E in CCT1) was also found in a previous study[15] to cause temperature sensitivity for growth under cold shock. The temperature sensitivity for growth at 15 °C is found to be least in the case of the MA6 and MA8 strains, with the latter growing similarly to the wild-type strain.

Effects of D→E mutations in CCT on cell morphology

Cells from midlogarithmic-phase cultures of the different strains were fixed and stained for actin and DNA (Fig. 3). The most striking phenotype is observed in the case of the MA2 strain. The volume of these cells is, on average, about six times larger than that of wild-type cells, suggesting a cell cycle defect. In addition, the MA2 cells are found to have many more actin patches, compared with the wild-type cells and all the other MA strains, and hardly any actin cables. The MA7 cells have unusually elongated buds and cell volumes that, on average, are 2-fold larger than those of wild-type cells. The MA5 cells are also found to be, on average, enlarged by a factor of about 2 and to have relatively more actin patches. All the other strains appear to be similar to the wild-type strain. However, fluorescence-activated cell sorting (FACS) cell cycle analysis (Fig. 3) shows that, in the case of the wild-type strain, the number of cells with one set (1*N*) of chromosomes and the number of cells with two sets (2*N*) of chromosomes are roughly equal, whereas in the case of all the mutant strains, except for MA2, the number of cells with 1*N* greatly exceeds the number of cells with 2*N*, thus indicating that they exit G1 more slowly or are under G1 arrest. Strikingly, in the case of the MA2 strain, we find that most cells are with 2*N*, and a minority of cells are with 4*N*. This finding is in accord with the much larger size of the MA2 cells. Halo assays showed that the MA2 cells were able to mate with their opposite type, thereby indicating that they have not become diploid and are only pseudo-diploid. In addition, mutating the MA2 strain back to the wild-type strain restored the wild-type phenotype, thus indicating that the mutation in CCT2 was not accompanied by other unintended mutations and that the MA2 strain did not become diploid.

Sensitivity of the growth of different MA cell strains to latrunculin-A and benomyl

Given the essential function of CCT in assisting the folding of actin and tubulin,[3,4] we tested the effects of latrunculin-A (an actin polymerization inhibitor) and benomyl (a β-tubulin polymerization inhibitor) on the growth of the different MA strains. The largest retarding effect of latrunculin-A on cell growth is seen in the case of the MA7 cells (Fig. 4a). Relatively large effects are also seen in the case of the MA2 and MA5 cells. The effects on the growth of the other mutant strains are much smaller and similar to the effect on the growth of the wild-type MA strain (with the exception of the MA6 cell strain, in which case an even smaller effect is observed). The greater sensitivity of MA2 and MA5 cells to latrunculin-A is in accord with a previous structural work[6] that showed that α-actin binds to CCT via subunits CCT4, CCT2, and CCT5. The very large effect of latrunculin-A seen in the case of the MA7 strain is unexpected but in line with our findings that the

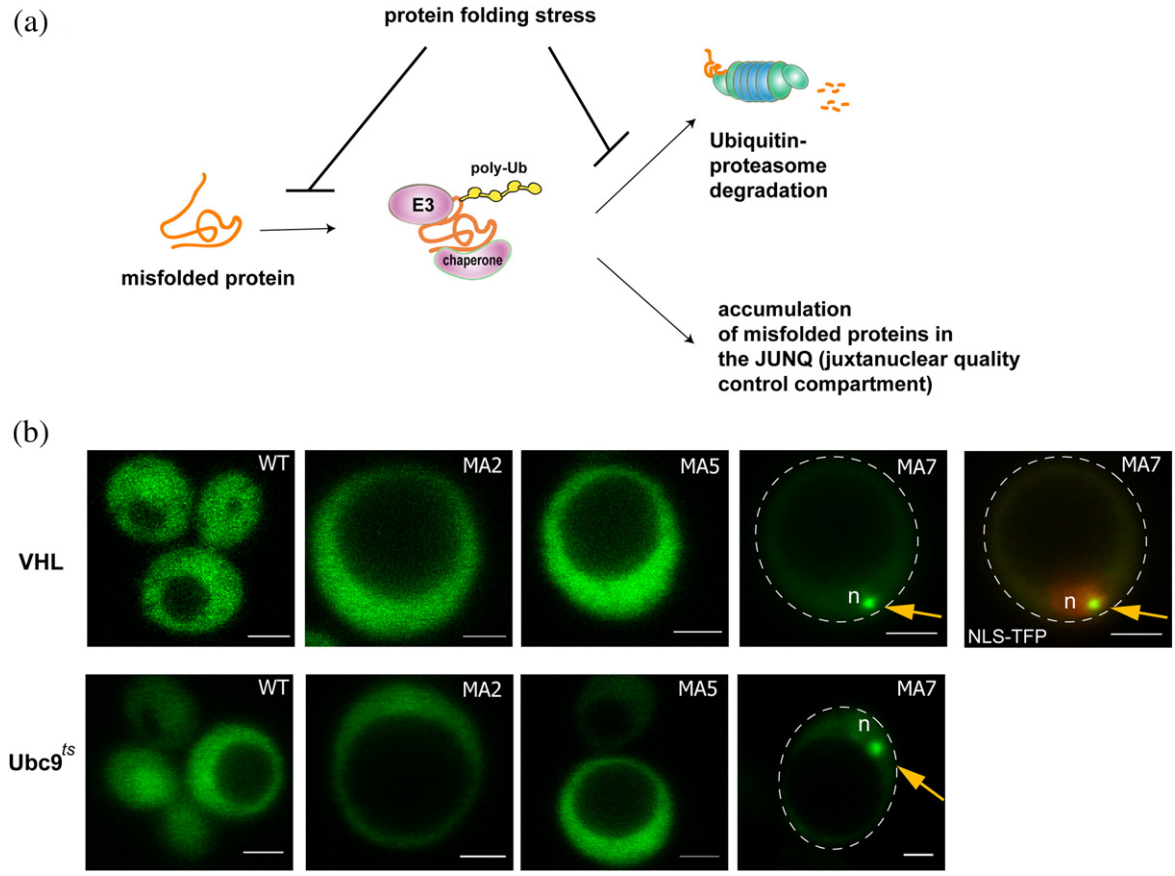

Fig. 5. The MA7 strain is the only strain that exhibits visually detectable signs of enhanced protein folding stress. (a) Enhanced protein folding stress overwhelms the quality control system and leads to accumulation of misfolded substrates in the juxtanuclear quality control compartment (JUNQ). (b) Accumulation of two misfolded GFP-fused substrates, VHL and Ubc9^{ts}, in the JUNQ is seen in the MA7 strain, but not in any of the other strains. In cells expressing GFP-VHL, nuclei were visualized by coexpressing NLS-tdTomato (NLS-TFP). Scale bar represents 2 μm.

MA2, MA5, and MA7 cells are those that display the most marked changes in cell shape and morphology (Fig. 3). The MA2, MA5, and, to a lesser extent, MA7 strains are also those that display the greatest sensitivity to benomyl (Fig. 4b). These results are also in agreement with previous structural and biochemical work[7] that showed that the interaction of CCT with tubulin involves subunits CCT2, CCT5, and CCT7. However, other subunits are also involved in the interaction of CCT with tubulin,[7] and the particular sensitivity of the MA2, MA5, and MA7 strains to benomyl might therefore be due to the fact that these strains are also impaired in actin folding and stress response (see the text below).

Effects of D→E mutations in CCT on protein aggregation *in vivo*

Protein aggregation in the different MA cells was monitored as described previously[16] using two green fluorescent protein (GFP)-fused model substrates: (i) Ubc9p^{ts},[17] a temperature-sensitive variant of the ubiquitin-conjugating (Ubc) enzyme Ubc9 that is a soluble nuclear protein misfolding at temperatures above 30 °C; and (ii) the von Hippel–Lindau (VHL) tumor suppressor, which folds only upon binding to its cofactor, elongin BC, and is known to be a CCT substrate.[18] Inclusions of GFP-VHL and GFP-Ubc9p^{ts} (at the borderline permissive temperature of 30 °C) were found to form only in the MA7 cells (Fig. 5). In these cells, juxtanuclear inclusions are formed as previously described,[16] whereas in all the other MA strains, including MA2 and MA5 (Fig. 5), no inclusions are observed, and GFP-VHL and GFP-Ubc9p^{ts} are seen to be diffuse.

Transcriptional analysis of gene expression in different MA strains

Microarray analysis of the whole *S. cerevisiae* yeast genome shows that the transcriptional response to the mutations in CCT varies considerably depending on which subunit was mutated (Fig. 6). Clustering analysis of differentially expressed genes in any of the mutant strains *versus* the wild-type strain (Fig. 6a) shows that the expression profiles of MA5 and, in particular, MA2 differ most, and that two pairs of strains—(i) MA1 and MA3, and (ii) MA6 and MA7—have similar profiles. The extent of similarity between every pair of strains was

quantified by calculating the Spearman's rank correlation coefficient ρ (Fig. 6b). It may be seen that the weakest correlations are indeed between the expression profile of MA2 and those of the other strains with ρ values that are between 0.5 and 0.65, and that the strongest correlation of MA2 is with MA5. By contrast, the ρ values for (i) MA1 and MA3 and (ii) MA6 and MA7 are 0.98 and 0.99, respectively. The extent of similarity between the different strains can also be determined using principal component analysis (Fig. 6c). Three components (designated components 1, 2, and 3) are found to account for about 95% of the variance in the data, with respective contributions of about 65%, 26%, and 4%. The MA2 strain differs from the wild-type strain mostly in the dimension (component) that accounts for 65% of the variance, whereas the other strains differ from the wild-type and MA2 strains in all three dimensions. It may also be seen again that the expression profiles of MA1 and MA6 are most similar to those of MA3 and MA7, respectively. Importantly, there are almost no significant changes in the transcription levels of the *CCT* genes themselves (except for the down-regulation of *CCT2* and *CCT3* in the MA2 and MA3 strains, respectively), thus suggesting, in conjunction with other results, that altered protein expression levels of the CCT complexes are unlikely to account for the observed phenotypes of the various strains.

The pseudo-diploid character of the MA2 strain is also reflected in the microarray data by the up-regulation (*versus* wild type) of the transcriptional response of genes involved in sporulation. For example, there is a significant [false discovery rate (FDR) <0.01] 7-fold increase in the transcription of SPO1, a meiosis-specific prospore protein, and a significant (FDR <0.004) 1.8-fold increase in the transcription of SPO11, a protein that initiates meiotic recombination. Overall, there is a very significant (adjusted $P < 10^{-4}$) enrichment in the

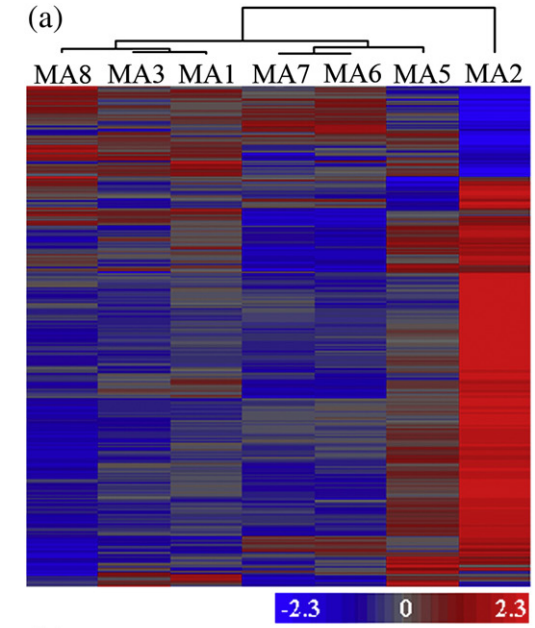

(b)

CCT subunit	8	3	2	6	5	1	7	4
8		0.95	0.52	0.90	0.86	0.95	0.92	NA
3	0.96		0.56	0.92	0.92	0.98	0.93	NA
2	0.52	0.57		0.59	0.65	0.58	0.52	NA
6	0.90	0.92	0.59		0.89	0.91	0.99	NA
5	0.86	0.92	0.65	0.90		0.93	0.89	NA
1	0.95	0.98	0.58	0.91	0.93		0.92	NA
7	0.92	0.93	0.59	0.99	0.89	0.92		NA
4	NA	NA	NA	NA	NA	NA	NA	

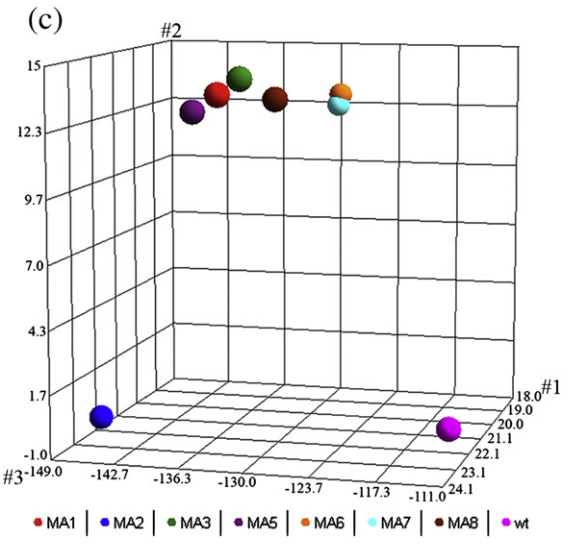

Fig. 6. Transcriptional response of *S. cerevisiae* yeast cells to the different mutations in CCT. (a) Clustered transcriptional expression profiles of the different MA strains using values of $\log_2(I_{mut}/I_{wt})$, where I_{wt} and I_{mut} are the standardized intensities of the wild-type and mutant MA strains. Data are shown only for those genes where a 2-fold change in $\log_2(I_{mut}/I_{wt})$ was found between at least two strains. Red and blue indicate increased and decreased values of $\log_2(I_{mut}/I_{wt})$ relative to the mean for each gene, in units of standard deviation. (b) Correlations between the expression profiles of the different strains. Spearman's rank correlation coefficient between the expression profiles of every pair of MA strains was calculated using the data in (a) (top half). In addition, it was calculated for every pair of strains when only genes where a 2-fold change in $\log_2(I_{mut}/I_{wt})$ was found relative to the wild-type strain were considered (bottom half). All correlations are extremely significant. The data are ordered in accordance with the order of subunits in the ring.[5] (c) Principal component analysis of the transcriptional expression profiles of the different strains. Principal component analysis was carried out using a covariance matrix generated from data on the intensities of expression of the wild-type and mutant MA strains using the same genes as in (a).

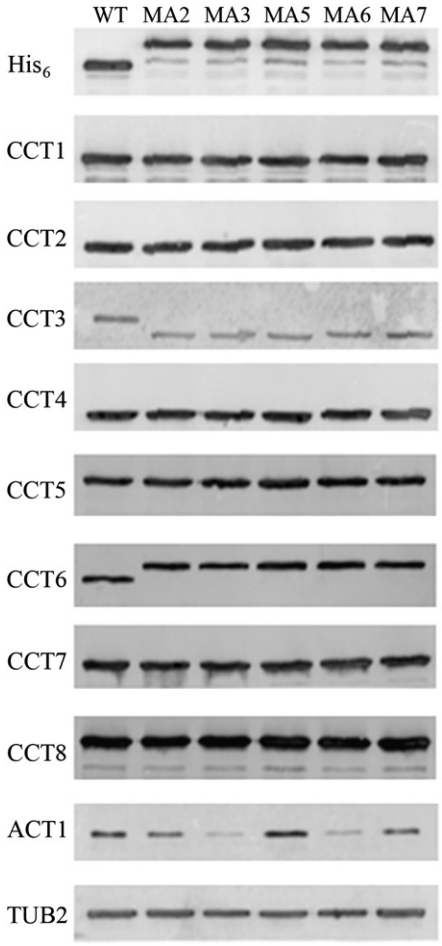

Fig. 7. *In vitro* analysis of CCT complexes. Western blot imaging of purified CCT complexes. Here, WT refers to the wild-type CCT complex in which the CBP tag (including a His_8-tag) is in subunit CCT3 and not in subunit CCT6.[19] CCT complexes purified from the MA2, MA3, MA5, MA6, and MA7 strains all carry the same CBP tag in subunit CCT6.[20] The two bottom panels were probed with anti-actin and anti-β-tubulin antibodies, as indicated.

GO term sporulation and in additional associated terms in the case of the MA2 strain, but not in the other strains.

In vitro characterization of the composition of CCT complexes purified from different MA strains

Western blot analysis using antibodies that are specific for the different CCT subunits shows that each of the subunits is present in the same amount in the CCT complexes purified from the different MA strains (Fig. 7). The presence of all eight subunits in the CCT complexes purified from the different MA strains was also confirmed by mass spectroscopy (data not shown). The Western blot analysis also shows that the presence of the calmodulin-binding peptide (CBP) tag in CCT3 (in the case of the wild-type strain) and in CCT6 (in the case of all the other strains) is reflected in the reduced electrophoretic mobility of the tagged subunits owing to their higher molecular weight. Taken together, these results indicate that proper assembly of the CCT complexes in the different MA strains is not affected by the D→E mutations. The Western blot analysis also shows that CCT purified from the different strains is able to bind actin and β-tubulin.

Discussion

The extent of 'individuality' of the different CCT subunits and a potential hierarchy in their functional roles were explored in this study by introducing, in each subunit in turn, the mutation D→E in the conserved GDGTTT ATP binding motif and by examining the resulting effects. A similar approach was described before,[21] but only some of the subunits of CCT were mutated in that study, and the mutations that were introduced were potentially disruptive and not identical. Remarkably, the relatively conservative (D→E) mutations in single subunits of the CCT complex described in the present study are found to have dramatic phenotypic consequences as we have also observed before[22] in the case of the G345D mutation in CCT4,[23] thereby indicating surprisingly little redundancy between subunits. A second striking observation in this study is that identical mutations in the different CCT subunits have such dramatically distinct effects, although the subunits cooperate in assisting folding.

What mechanism(s) is likely to be responsible for the diverse phenotypic effects of the mutations observed here? It is unlikely that the mutations block protein substrate binding, as indicated by the data for actin and tubulin in Fig. 7 and given that this step in the CCT reaction cycle is ATP independent.[3,4] Our results also indicate that proper assembly of the CCT complex is not impaired by the mutations (Fig. 7 and data not shown). It is more likely that the mutations interfere with substrate release and folding by affecting ATP hydrolysis†,[25]

† Steady-state kinetic analysis of the ATPase activity of several CCT mutant complexes was carried out; however, little, if any, differences between them were observed (data not shown). It should be realized, however, that knocking down the ATPase activity of a specific subunit can have a profound effect on its folding activity (as shown in this work) without it being reflected in the overall k_{cat} of the complex, as only one out of eight subunits is mutated at a time. Actin folding assays[24] at 30°C were also performed for several of the mutant CCT complexes (data not shown), which, in this respect, too, were all found to behave indistinguishably from wild-type CCT. Previously, however, we found that the G345D mutation in CCT4, which results in a much more severe actin phenotype *in vivo* at 30°C than any of those of the MA strains described here, reduces actin folding activity *in vitro* at 30°C only by a factor of 2.[22]

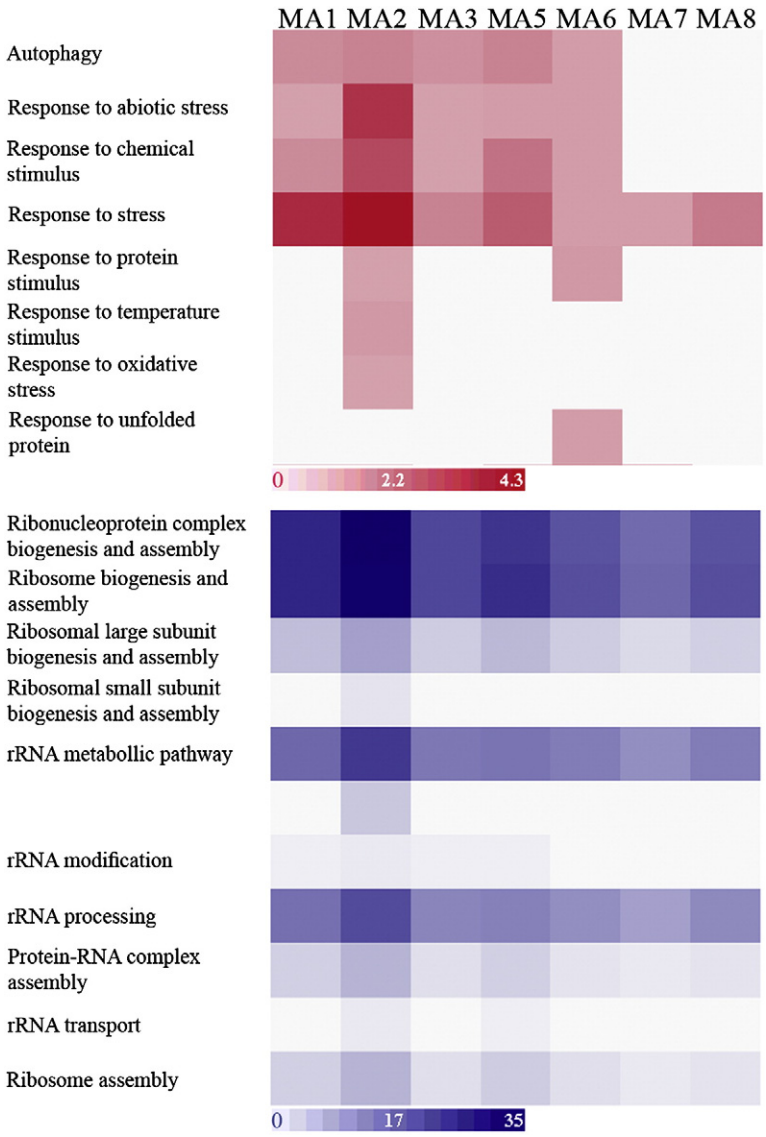

Fig. 8. Enrichment in up-regulated and down-regulated genes associated with stress-related processes and *de novo* protein synthesis, respectively, in the different MA strains. Red and blue indicate enriched processes for up-regulated and down-regulated genes, respectively. Heat maps correspond to minus the logarithm of the *P*-value for the significance of the enrichment. Functional annotation and statistical analyses were performed as described under Materials and Methods.

and that the diverse effects we observe therefore reflect subunit specificity for protein substrates. For example, it has been shown[6] that α-actin, which is an essential protein, interacts with CCT via subunits CCT4 and CCT2 or CCT5. Accordingly, we find here that the strain with the mutation in CCT4, the subunit involved in both modes of actin binding, is not viable, and that the MA2 and MA5 strains are those that grow slowest at 30 °C (Fig. 2), have the most altered transcriptional expression profiles (Fig. 6a), and are also sensitive to latrunculin A (Fig. 4a). The MA2 and MA5 strains also display sensitivity to benomyl (Fig. 4b), in accordance with previous observations that subunits CCT2 and CCT5 are the ones driving the high-affinity interaction between CCT and both α-tubulin and β-tubulin in the mammalian complex.[7] The MA7 and, to a much lesser extent, MA8 strains also display sensitivity to benomyl (Fig. 4b), in agreement with the observation that CCT7 and CCT8 have key roles in the modes of binding of the N-terminal domain of tubulin.[7] Our results are therefore in agreement with the finding that CCT2 and CCT5 are primary interactions sites for tubulin that function with CCT7 and CCT8, respectively, which are secondary interactions sites (Fig. 1). The key role of subunits CCT2 and CCT5 in the binding of both actin and tubulin may account for the finding here that the MA2 and MA5 strains are those that have the most altered transcriptional expression profiles (Fig. 6a). Subunit specificity in protein substrate binding may also explain, in part, the observation that GFP-VHL aggregates in MA7 cells (Fig. 5), as it has been shown[11] that VHL folding is mediated by subunits CCT7 and CCT1. Surprisingly, the MA7 strain is also extremely sensitive to latrunculin A (Fig. 4a) for reasons that appear to be only indirectly connected to the effect of the mutation on actin binding to CCT. The sensitivity of MA7 cells to benomyl, for example, may be due to toxic effects caused by inhibition of inclusion formation by this drug.[16] Alternatively, it may reflect a defect in the multidrug transporting system that renders these cells more sensitive to benomyl.

The phenotypic differences between the MA2 strain and the MA5 strain, despite the apparently equivalent roles of CCT2 and CCT5 in actin and tubulin folding, indicate that some functions of these subunits are not shared. For example, a recently reported[26] indication for a potentially unique role of CCT2 is the finding that it is a downstream phosphorylation target of the PI3-K–mTOR pathway. Interestingly, the CCT6 subunit has also been linked to the TOR pathway, as it was found that overexpression of this subunit suppresses the lethality of a *TOR2* mutation in yeast.[27,28] The TOR proteins in *S. cerevisiae*, Tor1p and Tor2p, exist as part of two complexes, TORC1 and TORC2, that regulate cell growth in response to environmental cues.[29] In particular, TORC2 was shown to be involved in the organization of the actin cytoskeleton in *S. cerevisiae*.[27] Given the (i) reported link[26] between the TOR pathway and CCT2, and the (ii) phenotype of the MA2 strain that shows impairment in cell growth processes regulated by the TOR pathway (Figs. 2 and 3), it occurred to us that the phenotype of the MA2 strain may, in part, reflect inhibition of the TOR pathway in these cells. Inhibition of the TOR pathway by rapamycin treatment is known to induce a stress response that is mediated by the Msn2/4 transcription factor.[30] Our microarray data show a significant (FDR <0.01) 2.5-fold increase in the transcription of Msn4 in the MA2 strain and no change in any of the other strains. Inhibition of the TOR pathway is also caused by elevated expression of targets of the Hsf1 transcription factor such as *PIR3* and *YRO2*.[31] Inspection of our microarray data shows an increased transcriptional expression of Hsf1 targets only in the MA2 cells. In particular, transcription levels of *PIR3* and *YRO2* are increased significantly (FDR <0.01) by 28-fold and 4-fold, respectively, in the MA2 strain and only much less in all the other strains. Finally, it has been shown[32] that the lethality of *tor2*Δ cells is suppressed by the D239A mutation in YPK2, an effector protein that in its phosphorylated state is involved in TORC2-mediated regulation of various processes such as actin organization. Here, we find that the transcription of *YPK2* is increased significantly (FDR <0.01) by a factor of 5 in MA2 cells and by a factor of 2 in MA5 cells, but not in any of the other strains. Taken together, our results indicate that the phenotype of the MA2 cells reflects, in part, suppression of TORC2-mediated signaling by the mutation D90E in CCT2. CCT2 in the CCT complex may be involved in mediating the folding of proteins that regulate or form the TORC2 complex, or may function outside of the CCT complex perhaps as a component of the TORC2 complex. The function of CCT2 outside of the CCT complex may be impaired owing to the down-regulation of the transcription of this gene in the MA2 cells. In addition, several components of the protein phosphatase 2A machinery interact with CCT; TAP42, SIT4, and WD40 regulators such as CDC55,[33] and one or more of these components may be more strongly affected in MA2 cells.

The MA7 strain was the only strain found to contain aggregates of the GFP fusions of VHL and Ubc9p^{ts} (Fig. 5). The juxtanuclear localization of these aggregates indicates that quality control of these substrates in MA7 cells is not impaired at the level of ubiquitination, as this is also a major site of proteasome concentration.[16] As mentioned above, subunit specificity in protein substrate binding may explain, in part, the observation that GFP-VHL aggregates in MA7 cells, since it has been shown[11] that VHL folding is mediated by subunits CCT7 and CCT1. Interrogation of the microarray data reveals, however, that a more general mechanism may be responsible for the aggregation phenomena in the MA7 strain. It has been suggested that response to stress in eukaryotes involves induction of chaperones that protect the cell from stress and repression of other chaperones involved in protein synthesis.[34] In other words, aggregation is more likely to occur when misfolding is neither prevented by slowing protein synthesis nor reversed by chaperone action. Our data show that both the up-regulated response to stress and the down-regulation of processes related to protein synthesis are weakest in the MA7 strain (Fig. 8), thereby helping to explain why aggregates are observed only in this strain.

Several recent studies have reported that overexpression of a specific CCT subunit can suppress the deleterious effects of mutations in other genes. For example, as mentioned above, overexpression of CCT6 suppresses the lethality of a *TOR2* mutation in yeast.[27,28] It is therefore intriguing that overexpression of CCT7 was recently reported to alleviate a defect in the septum machinery in the *slt2*Δ *rim101*Δ mutant,[35] given that only MA7 cells were found here to have elongated buds (Fig. 3). Mutations in other CCT subunits affect GFP-septin localization in cells,[20] but do not cause the altered cell morphology observed here in MA7. Taken together, our data support the notion that individual subunits of CCT engage in 'moonlighting' functions in addition to their core actin and tubulin folding activities. Replacing a chromosomal CCT gene with a plasmid-encoded one, as has been performed in some structure–function studies, may therefore result in unintended phenotypic effects due to excess subunits that fail to incorporate into the CCT complex and instead affect other cellular processes.

In summary, this study shows that the different subunits of CCT have unique roles that are related to subunit-specific substrate specificity and possibly also to special 'moonlighting' functions they might be involved in as individual subunits and not as part of the full complex. The most dramatic phenotypic effects we observe are associated with the mutations in CCT2, CCT5, and CCT7. It remains to be determined whether the rank order of magnitude of effects also reflects in some way the sequential pathway(s) of allosteric changes within and between rings.[10] It is of interest in this regard that several pairs of subunits that are most similar to each other in their transcriptional response to the mutation (Fig. 6b) are also neighbors that form direct intra-ring

interactions (CCT3/CCT8) or close inter-ring interactions (CCT2/CCT5 and CCT1/CCT3).

Materials and Methods

Molecular biology

The chromosomal *CCT6* gene in the haploid strain of *S. cerevisiae* yeast (strain BJ2168) was replaced with a copy containing an in-frame insertion of the coding sequence for CBP, followed by a selectable marker (KanR) downstream of the gene, as previously described.[20] The genotype of this strain that is referred to in this study as wild type is *Mat a leu2, trp1, gal2, ura3-52, leu2-3, prb1-1122, pep4-3, prc467, CCT6*: :*CBP*: :*KanMX4*. Replacement of *KanMX4* in this strain with the URA3-selectable marker yielded a second strain that is referred to below as the MA strain. The strain with the mutation D89E in CCT6, designated MA6, was generated using homologous recombination by transforming BJ2168 cells with a fragment derived from pET17b, which contains the gene for *CCT6-CBP* (with the mutation), followed upstream by the kanamycin resistance cassette and the gene's 3′ untranslated region (UTR). The strains with mutation D96E in CCT1, mutation D90E in CCT2, mutation D91E in CCT3, mutation D91E in CCT4, mutation D117E in CCT5, or mutation D96E in CCT7, designated MA1, MA2, MA3, MA4, MA5, and MA7, respectively, were generated using homologous recombination by transforming MA cells with a pET17b-derived fragment containing the respective mutant gene, followed by the kanamycin resistance cassette and the gene's 3′ UTR. The strain with the mutation D98E in CCT8, designated MA8, was generated similarly by transforming MA cells with a pUC19-derived fragment containing the mutant *CCT8* gene (without the first 150 bases), followed by the kanamycin resistance cassette and the gene's 3′ UTR. All the strains, except for MA4, were found to be viable. A silent mutation at position 91 in CCT4 resulted in a viable strain, thereby indicating that the mutation D91E in CCT4 is responsible for the loss of viability. All the mutations were introduced using the Invitrogen site-directed mutagenesis kit. Colonies were screened for mutations on YPD plates containing 300 μg/ml geneticin, and the presence of the desired mutation was then verified by direct sequencing of the full gene. The MA2 strain was converted back to a wild-type-like strain by transforming MA2 cells with a fragment containing the gene for wild-type CCT2, followed by the LEU2 marker and the gene's 3′ UTR. In this case, colonies were screened on SC-Leu (synthetic complete without Leu) plates containing 2% wt/vol dextrose. The sequences of all the primers used in this work are available upon request.

Growth assays

Cultures of the different yeast strains that were grown overnight at 30 °C were diluted to an OD of about 0.5 and then grown for another 5–7 h. The cultures were then diluted again to an OD of 0.5, and a series of nine 2-fold dilutions of each culture was prepared in a sterile 96-well plate. Drops of 2 μl from each well in the plate were transferred with a multiblot (V&P Scientific, Inc., San Diego, CA) onto square YPD plates containing 300 μg/ml geneticin (or 15 μg/ml benomyl, when appropriate). The plates were incubated at 15, 30, or 37 °C for 8, 3, or 4 days, respectively, and then photographed with a GelDoc XR camera (Bio-Rad). The effects of latrunculin-A on cell growth were monitored using a halo assay, as described previously.[36] A 10-μl culture of cells in logarithmic phase mixed with 4 ml of warm YPD agar media was added to each YPD plate. A sterile concentration disk (Becton Dickinson) soaked in dimethyl sulfoxide containing 0 or 1 mM latrunculin-A was then placed on each plate. The plates were incubated at 30 °C for 48 h and then photographed. All the experiments were carried out at least in duplicate.

Fluorescence microscopy

Cultures inoculated from fresh 5-ml starters were grown in 50 ml of YPD containing 300 μg/ml geneticin in 250-ml flasks at 30 °C with shaking at 250 rpm until the early logarithmic phase. Cells were fixed by addition of 5 ml of 37% wt/vol paraformaldehyde to 45 ml of the culture and by incubation for 10 min at room temperature. The cells were then centrifuged, resuspended in phosphate-buffered saline (PBS) with 4% wt/vol paraformaldehyde, and incubated for 1 h at room temperature. Following three washes with PBS, the cells were permeabilized by incubating them in PBS containing 0.25% Triton X-100 and 2.5% bovine serum albumin for 15 min at room temperature. The cells were then washed again three times in PBS and stained for actin by incubating them in PBS containing 10 μl of 0.7 μM Alexa Fluor 488 phalloidin and 2.5% bovine serum albumin for 1 h in the dark at room temperature. Following three washes in PBS, the cells were resuspended in 30 μl of PBS, and droplets of the labeled cells were applied to a microscope slide with mounting medium in the presence of 0.75 μg/ml 4′,6-diamidino-2-phenylindole. Slides were then examined at room temperature using a Deltavision microscope (Applied Precision), with lasers exciting at 353 and 488 nm. Multicolor images were collected sequentially in 0.2-μm sections in two channels with a ×100 lens. The images were chromatically corrected and deconvoluted with the Softworx software, and a final image was created using the quick projection feature.

Fluorescence-activated cell sorting

Cells were fixed with 70% ethanol, washed twice with 50 mM Tris–HCl (pH 8.0) (buffer A), and then treated with 1 mg/ml RNase A for 40 min at 37 °C. Following two washes with buffer A, the cells were treated with 20 mg/ml proteinase K for 1 h at 37 °C, washed again with buffer A, and then incubated with 1:1000 SYBR Green I (Molecular Probes) in 200 μl of buffer A for 1 h at room temperature. The cells were then centrifuged, resuspended in 300 μl of buffer A, sonicated for 5 s, and transferred to FACS tubes. The fluorescence of 100,000 cells of each strain was measured using an LSR II flow cytometer system (Becton Dickinson) with excitation and emission wavelengths of 488 and 530 nm, respectively. Data were analyzed with FCS Express (De Novo Software).

Monitoring of protein aggregation *in vivo*

The different MA cell strains were transformed with the previously described[16] plasmids pESC-LEU GFP-Ubc9^{ts} and pESC-LEU GFP-VHL NLS-tdTomato. Following transformation, the cells were grown at 30 °C on agar plates with SC-Leu media containing 2% sucrose, 2% raffinose, and 2% glucose to repress the transcription of

the GFP fusion proteins (controlled by the GAL promoter). Single colonies were then picked and grown in 75 ml of liquid SC-Leu media containing 2% sucrose, 2% raffinose, and 2% galactose to induce the expression of the exogenous gene. Cells were grown until they had reached an OD of 0.5–1 and diluted 2-fold, and 100 μl of this dilution was then placed on a glass-bottom 35-mm dish (MatTek Corp.). Cells were imaged as soon as they had settled on the plate (approximately 5 min later). Confocal images were taken with a Zeiss LSM 710 laser-scanning microscope using a ×63 oil objective, a 488-nm laser, and a 1-μm pinhole. Images were processed with Zeiss LSM Image Browser software.

Microarray analysis

Overnight cultures of the wild-type strain and each of the MA strains were diluted appropriately and then grown at 30 °C until an OD of 0.5 had been reached. The cells were then pelleted by centrifugation for 1 min at 600*g*, flash frozen at −80 °C in liquid N_2, and stored at −80 °C until use. Total RNA was purified using the MasterPure Yeast RNA purification kit (Epicentre Biotechnologies). Total RNA from each strain was purified from two independent cultures and analyzed separately. cDNA was prepared by reverse transcribing the total RNA that was purified using a T7-oligo(dT) primer and reverse transcriptase, thereby generating the first strand. The second strand was synthesized by adding RNase H to the DNA–RNA hybrid and filling in the gaps created in the RNA strand using DNA polymerase I. The purified cDNA was then transcribed by RNA polymerase in the presence of a biotinylated nucleotide analog. The biotinylated RNA was cleaned up, fragmented, and hybridized to the GeneChip Yeast Genome 2.0 array (Affymetrix, Inc., Santa Clara, CA) for 16 h at 45 °C, with shaking. The arrays were then washed, incubated with phycoerythrin-labeled streptavidin, and washed again. The chips were scanned using a GeneChip 3000 scanner (Affymetrix, Inc.).

Transcriptome analysis was carried out using Partek Genome Suite software‡ (Partek, Inc., St. Louis, MO 63141). CEL files (containing raw expression measurements) were imported to Partek GS. Preprocessing was carried out using the Robust Microarray Averaging algorithm.[37] One-way ANOVA was performed. FDR was applied to correct for multiple comparisons.[38] Differentially expressed genes were chosen according to FDR <0.05, and that there is at least a 2-fold change between the mutated strain and the wild type. Exploratory principal component analysis was carried out using Partek (covariance matrix was calculated, and eigenvectors were normalized). Clustering analysis was performed using Pearson's dissimilarity and complete linkage. Functional annotation analysis was performed using the Fatiscan tool available in the Babelomics v3.2 web site‖.[39,40]

In vitro characterization of the composition of different CCT complexes

CCT was purified from cultures of the different yeast strains, as described previously.[19,22] The presence of all eight different subunits in the purified complexes was verified by Typhoon Western blot imaging of 5 μg of the different purified CCT complexes after electrophoresis on 10% SDS-PAGE. Imaging was carried out using ECL Plus and anti-peptide antibodies against the eight CCT subunits or antibodies against yeast actin (ACT1), β-tubulin (TUB2), or the His_8-tag.[19] The rabbit anti-CCT subunit antibodies and the rat anti-ACT1 monoclonal antibody were produced and used as described previously.[24] The rabbit anti-TUB2 antibody was raised against the C-terminal peptide APQNQDEPITENFE. The presence of all eight different subunits in the purified complexes was also confirmed by electrospray ionization tandem mass spectrometry analysis of tryptic cleavage-derived peptide mixtures separated by online reverse-phase nanoscale capillary liquid chromatography. Steady-state ATPase assays were carried out as described previously[22,41] at 25 °C in 50 mM Tris–HCl buffer (pH 7.5) containing 10 mM $MgCl_2$, 50 mM KCl, 2 mM DTT, and 20% (vol/vol) glycerol.

‡ http://www.partek.com
‖ http://babelomics.bioinfo.cipf.es/

Acknowledgements

We thank Dr. Hagai Abeliovich, Dr. Ghil Jona, and Gillian Hynes for helpful advice, and Dr. Yoav Peleg for help with the cloning of the *CCT8* gene. M.A. received a short-term EMBO fellowship. This work was supported by grant 153/08 from the Israel Science Foundation (A.H.) and by Cancer Research UK (K.R.W.). A.H. is an incumbent of the Carl and Dorothy Bennett Professorial Chair in Biochemistry.

References

1. Horwich, A. L., Weber-Ban, E. U. & Finley, D. (1999). Chaperone rings in protein folding and degradation. *Proc. Natl Acad. Sci. USA*, **96**, 11033–11040.
2. Horwich, A. L., Fenton, W. A., Chapman, E. & Farr, G. W. (2007). Two families of chaperonin: physiology and mechanism. *Annu. Rev. Cell Dev. Biol*, **23**, 115–145.
3. Spiess, C., Meyer, A. S., Reissmann, S. & Frydman, J. (2004). Mechanism of the eukaryotic chaperonin: protein folding in the chamber of secrets. *Trends Cell Biol.* **14**, 598–604.
4. Valpuesta, J. M., Carrascosa, J. L. & Willison, K. R. (2005). Structure and function of the cytosolic chaperonin CCT. In *Protein Folding Handbook* (Buchner, J. & Kiefhaber, T., eds), pp. 725–755, Wiley-VCH, Weinheim, Germany.
5. Liou, A. K. F. & Willison, K. R. (1997). Elucidation of the subunit orientation in CCT (chaperonin containing TCP1) from the subunit composition of CCT micro-complexes. *EMBO J.* **16**, 4311–4316.
6. Llorca, O., McCormack, E. A., Hynes, G., Grantham, J., Cordell, J., Carrascosa, J. L. *et al.* (1999). Eukaryotic type II chaperonin CCT interacts with actin through specific subunits. *Nature*, **402**, 693–696.
7. Llorca, O., Martín-Benito, J., Ritco-Vonsovici, M., Grantham, J., Hynes, G. M., Willison, K. R. *et al.* (2000). Eukaryotic chaperonin CCT stabilizes actin and tubulin folding intermediates in open quasi-native conformations. *EMBO J.* **19**, 5971–5979.
8. Cong, Y., Baker, M. L., Jakana, J., Woolford, D., Miller, E. J., Reissmann, S. *et al.* (2010). 4.0-Å resolution cryo-EM structure of the mammalian chaperonin TRiC/CCT reveals its unique subunit arrangement. *Proc. Natl Acad. Sci. USA*, **107**, 4967–4972.

9. Martin-Benito, J., Grantham, J., Boskovic, J., Brackley, K. I., Carrascosa, J. L., Willison, K. R. & Valpuesta, J. M. (2007). The inter-ring arrangement of the cytosolic chaperonin CCT. *EMBO Rep.* **8**, 252–257.
10. Rivenzon-Segal, D., Wolf, S. G., Shimon, L., Willison, K. R. & Horovitz, A. (2005). Sequential ATP-induced allosteric transitions of the cytoplasmic chaperonin containing TCP-1 revealed by EM analysis. *Nat. Struct. Mol. Biol.* **12**, 233–237.
11. Spiess, C., Miller, E. J., McClellan, A. J. & Frydman, J. (2006). Identification of the TriC/CCT substrate binding sites uncovers the function of subunit diversity in eukaryotic chaperonins. *Mol. Cell*, **24**, 25–37.
12. Ditzel, L., Löwe, J., Stock, D., Stetter, K. O., Huber, H., Huber, R. & Steinbacher, S. (1998). Crystal structure of the thermosome, the archaeal chaperonin and homolog of CCT. *Cell*, **93**, 125–138.
13. Weiss, C. & Goloubinoff, P. (1995). A mutant at position 87 of the GroEL chaperonin is affected in protein binding and ATP hydrolysis. *J. Biol. Chem.* **270**, 13956–13960.
14. Leroux, M. R. & Hartl, F. U. (2000). Protein folding: versatility of the cytosolic chaperonin TRiC/CCT. *Curr. Biol.* **10**, R260–R264.
15. Ursic, D., Sedbrook, J. C., Himmel, K. L. & Culberston, M. R. (1994). The essential yeast TCP1 protein affects actin and microtubules. *Mol. Biol. Cell*, **5**, 1065–1080.
16. Kaganovich, D., Kopito, R. & Frydman, J. (2008). Misfolded proteins partition between two distinct quality control compartments. *Nature*, **454**, 1088–1095.
17. Betting, J. & Seufert, W. (1996). A yeast Ubc9 mutant protein with temperature-sensitive *in vivo* function is subject to conditional proteolysis by a ubiquitin- and proteasome-dependent pathway. *J. Biol. Chem.* **271**, 25790–25796.
18. Feldman, D. E., Thulasiraman, V., Ferreyra, R. G. & Frydman, J. (1999). Formation of the VHL–elongin BC tumor suppressor complex is mediated by the chaperonin TRiC. *Mol. Cell*, **4**, 1051–1061.
19. Pappenberger, G., McCormack, E. A. & Willison, K. R. (2006). Quantitative actin folding reactions using yeast CCT purified via an internal tag in the CCT3/γ subunit. *J. Mol. Biol.* **360**, 484–496.
20. Dekker, C., Stirling, P. C., McCormack, E. A., Filmore, H., Paul, A., Brost, R. L. *et al.* (2008). The interaction network of the chaperonin CCT. *EMBO J.* **27**, 1827–1839.
21. Lin, P. & Sherman, F. (1997). The unique hetero-oligomeric nature of the subunits in the catalytic cooperativity of the yeast CCT chaperonin complex. *Proc. Natl Acad. Sci. USA*, **94**, 10780–10785.
22. Shimon, L., Hynes, G. M., McCormack, E. A., Willison, K. R. & Horovitz, A. (2008). ATP-induced allostery in the eukaryotic chaperonin CCT is abolished by the mutation G345D in CCT4 that renders yeast temperature-sensitive for growth. *J. Mol. Biol.* **377**, 469–477.
23. Vinh, D. B. N. & Drubin, D. G. (1994). A yeast TCP-1-like protein is required for actin function *in vivo*. *Proc. Natl Acad. Sci. USA*, **91**, 9116–9120.
24. McCormack, E. A., Altschuler, G. M., Dekker, C., Filmore, H. & Willison, K. R. (2009). Yeast phosducin-like protein 2 acts as a stimulatory co-factor for the folding of actin by the chaperonin CCT via a ternary complex. *J. Mol. Biol.* **391**, 192–206.
25. Meyer, A. S., Gillespie, J. R., Walther, D., Millet, I. S., Doniach, S. & Frydman, J. (2003). Closing the folding chamber of the eukaryotic chaperonin requires the transition state of ATP hydrolysis. *Cell*, **113**, 369–381.
26. Abe, Y., Yoon, S. O., Kubota, K., Mendoza, M. C., Gygi, S. P. & Blenis, J. (2009). p90 ribosomal S6 kinase and p70 ribosomal S6 kinase link phosphorylation of the eukaryotic chaperonin containing TCP-1 to growth factor, insulin, and nutrient signaling. *J. Biol. Chem.* **284**, 14939–14948.
27. Schmidt, A., Kunz, J. & Hall, M. N. (1996). TOR2 is required for organization of the actin cytoskeleton in yeast. *Proc. Natl Acad. Sci. USA*, **93**, 13780–13785.
28. Kabir, M. A., Kaminska, J., Segel, G. B., Bethlendy, G., Lin, P., Della Seta, F. *et al.* (2005). Physiological effects of unassembled chaperonin Cct subunits in the yeast *Saccharomyces cerevisiae*. *Yeast*, **22**, 219–239.
29. Jacinto, E. (2008). What controls TOR? *IUBMB Life*, **60**, 483–496.
30. Beck, T. & Hall, M. N. (1999). The TOR signalling pathway controls nuclear localization of nutrient-regulated transcription factors. *Nature*, **402**, 689–692.
31. Bandhakavi, S., Xie, H., O'Callaghan, B., Sakurai, H., Kim, D. H. & Griffin, T. J. (2008). Hsf1 activation inhibits rapamycin resistance and TOR signaling in yeast revealed by combined proteomic and genetic analysis. *PLoS One*, **3**, e1598.
32. Kamada, Y., Fujioka, Y., Suzuki, N. N., Inagaki, F., Wullschleger, S., Loewith, R. *et al.* (2005). Tor2 directly phosphorylates the AGC kinase Ypk2 to regulate actin polarization. *Mol. Cell. Biol.* **25**, 7239–7248.
33. Glatter, T., Wepf, A., Aebersold, R. & Gstaiger, M. (2009). An integrated workflow for charting the human interaction proteome: insights into the PP2A system. *Mol. Syst. Biol.* **5**, 237.
34. Albanèse, V., Yam, A. Y., Baughman, J., Parnot, C. & Frydman, J. (2006). Systems analyses reveal two chaperone networks with distinct functions in eukaryotic cells. *Cell*, **124**, 75–88.
35. Gomez, A., Perez, J., Reyes, A., Duran, A. & Roncero, C. (2009). Slt2 and Rim101 contribute independently to the correct assembly of the chitin ring at the budding yeast neck in *Saccharomyces cerevisiae*. *Eukaryotic Cell*, **8**, 1449–1459.
36. Ayscough, K. (1998). Use of latrunculin-A, an actin monomer-binding drug. *Methods Enzymol.* **298**, 18–25.
37. Irizarry, R. A., Hobbs, B., Collin, F., Beazer-Barclay, Y. D., Antonellis, K. J., Scherf, U. & Speed, T. P. (2003). Exploration, normalization, and summaries of high density oligonucleotide array probe level data. *Biostatistics*, **4**, 249–264.
38. Hochberg, Y. & Benjamini, Y. (1990). More powerful procedures for multiple significance testing. *Stat. Med.* **9**, 811–818.
39. Al-Shahrour, F., Minguez, P., Tárraga, J., Montaner, D., Alloza, E., Vaquerizas, J. M. *et al.* (2006). BABELOMICS: a systems biology perspective in the functional annotation of genome-scale experiments. *Nucleic Acids Res.* **34**, W472–W476.
40. Al-Shahrour, F., Arbiza, L., Dopazo, H., Huerta-Cepas, J., Minguez, P., Montaner, D. & Dopazo, J. (2007). From genes to functional classes in the study of biological systems. *BMC Bioinf.* **8**, *114.*
41. Brune, M., Hunter, J. L., Corrie, J. E. & Webb, M. R. (1994). Direct, real-time measurement of rapid inorganic phosphate release using a novel fluorescent probe and its application to actomyosin subfragment 1 ATPase. *Biochemistry*, **33**, 8262–8271.